

## International Journal of Bio-Inorganic Hybrid Nanomaterials

### Magnetic Nanoporous Silica as Carriers for Ibuprofen: Adsorption and Release Study

Alireza Badiel<sup>1\*</sup>, Zohreh Bahrami<sup>2</sup>, Ali Jahangir<sup>3</sup> and Ghodsi Mohammadi Ziarani<sup>4</sup>

<sup>1</sup> Professor, School of Chemistry, College of Science, University of Tehran, Tehran, Iran & Nanobiomedicine Center of Excellence, Nanoscience and Nanotechnology Research Center, University of Tehran, Tehran, Iran

<sup>2</sup> Ph.D., School of Chemistry, College of Science, University of Tehran, Tehran, Iran

<sup>3</sup> M.Sc., School of Chemistry, College of Science, University of Tehran, Tehran, Iran

<sup>4</sup> Professor, Research Laboratory of Pharmaceutical, Alzahra University, Vanak, Tehran, Iran

Received: 11 March 2014; Accepted: 14 May 2014

#### ABSTRACT

A carrier system based on nanoporous silica (SBA-15) with magnetic nanoparticles of  $\text{CoFe}_2\text{O}_4$  was synthesized via the impregnation of cobalt salt, iron salt and citric acid with as-synthesized SBA-15. The obtained samples were characterized by small angle X-ray scattering (SAXS),  $\text{N}_2$  adsorption/desorption, scanning electron microscopy (SEM), vibrating sample magnetometer (VSM) and ultraviolet (UV) spectroscopy. The effect of magnetization on the drug release behavior of SBA-15 has been studied. Ibuprofen was chosen as a model drug. Drug release studies in simulated body fluid (SBF) at pH 7.4 showed that after 48 hours, the percentage of drug release through SBA-15 and magnetic SBA-15 could reach up to 80% and 20%, respectively. The obtained results reveal that the magnetization leads towards significant decrease of the drug release rate.

**Keyword:** SBA-15;  $\text{CoFe}_2\text{O}_4$ ; Ibuprofen; Drug release; Magnetism.

## 1. INTRODUCTION

Design of drug carrier systems (DDS) based on magnetic nanoparticles is one of the attractive research field because it provides the ability to guiding the drugs to the position of interest in the presence of an external magnetic field [1]. Among the several matrixes that can be used in this area such as polymer micelles [2, 3] and lipid vesicles [4], highly ordered mesoporous silica materials have gained considerable attention for following properties: high surface areas, tunable pore sizes and volumes, and well-defined surface properties for modification [5-7]. Up to now, the research relating

to the application of magnetic mesoporous silica materials as carriers for drug delivery has been reported by many groups [8-14]. Synthesis of spherical silica-based mesoporous materials encapsulating magnetic  $\text{Fe}_2\text{O}_3$  nanoparticles and investigation of their potential for drug targeting were described by Vallet-Regi et al. [9]. Hyeon's group reported using uniform mesoporous silica spheres embedded with magnetic nanocrystals as magnetic fluorescent delivery vehicles [10].

The aim of this work is the synthesis of magnetically functionalized SBA-15 with  $\text{CoFe}_2\text{O}_4$  nanoparticles

(\* ) Corresponding Author - e-mail: abadiel@khayam.ut.ac.ir

and study of its potential application as carrier in drug delivery system. Ibuprofen (IBU) was chosen as a model drug to evaluate the storage capacity and delivery profiles of the non-modified and magnetically functionalized SBA-15.

## 2. EXPERIMENTAL

### 2.1. Materials

Poly (ethylene glycol) block poly (propylene glycol) block poly (ethylene glycol), P123, (EO<sub>20</sub>PO<sub>70</sub>EO<sub>20</sub>, M<sub>w</sub>= 5800 g/mol) was purchased from Aldrich. Tetraethyl orthosilicate (TEOS), hydrochloric acid (37%), cobalt (II) nitrate hexahydrate, iron (III) chloride hexahydrate, citric acid and n-hexane were obtained from Merck. Ibuprofen was purchased from Sigma-Aldrich. All chemical reagents were used without further purification.

#### 2.1.1. Characterization

Small angle X-ray scattering (SAXS) patterns were recorded with a model Hecus S3-MICROpix SAXS diffractometer with a one-dimensional PSD detector using Cu K $\alpha$  radiation (50 kV, 1mA) at wavelength 1.54 Å. The scanning electron microscopy (SEM) images were obtained on Oxford LEO 1455V STEM and Philips EM-208 100 KV, respectively. The N<sub>2</sub> adsorption/desorption measurements were conducted at liquid nitrogen temperature (77 K) using BELSORP-mini II. The specific surface areas were measured using multiple point Brunauer-Emmett-Teller (BET) method. The pore size distributions were calculated using desorption branches of the isotherms by Barrett-Joyner-Halenda (BJH) method. The magnetic properties of sample were measured by MeghnatisDaghig-Kavir Co., vibrating sample magnetometer (VSM) at room temperature. The ultraviolet (UV) absorption spectra were obtained using a Raylight, UV 1600 spectrophotometer.

### 2.2. Methods

#### 2.2.1. Synthesis of SBA-15

Mesoporous silica SBA-15 was synthesized according to the procedure that described in our previous work [15]. In a typical synthesis, 4 g of nonionic triblock

copolymer (PluronicP123) was dissolved in the mixture of deionized water (30 g) and hydrochloric acid (120 g, 2M). 8.54 g of TEOS was added to the homogeneous solution under stirring. The produced gel was aged at 40°C for 24 h and heated to 100°C for 48 h. The solid product was obtained after filtration and then calcination at 600°C for 6 h.

#### 2.2.2. Preparation of magnetically functionalized SBA-15

The magnetically functionalized SBA-15 was prepared by the procedure reported in the literature [16]. 1 g of as-synthesized SBA-15 was dispersed into 20 mL of anhydrous ethanol, followed by addition of cobalt salt (Co(NO<sub>3</sub>)<sub>2</sub>·6H<sub>2</sub>O), iron salt (FeCl<sub>3</sub>·6H<sub>2</sub>O) and citric acid. The ratios of Fe(III) to Co(II) and citric acid to Fe(III) were fixed at 2.0. After stirring at room temperature for complete evaporation of ethanol, the residual solid was dried at 80°C for overnight, followed by calcination at 550°C for 10 h. The final sample was denoted as M-SBA-15.

#### 2.2.3. Drug loading

Ibuprofen was chosen as a model drug to evaluate the loading and release behavior of SBA-15 and the magnetically functionalized SBA-15. The loading of ibuprofen inside the SBA-15 and M-SBA-15 was carried out as in the following way: 0.3 g of the sample was added to 20 mL of ibuprofen-hexane solution (35 mg·mL<sup>-1</sup>) and soaked under stirring at room temperature for 24 h to reach the equilibrium state. Finally, the precipitate was filtered and washed thoroughly with hexane, dried under vacuum at 40°C. The obtained samples were designated as IBU@SBA-15 and IBU@M-SBA-15. The amount of loaded drug was determined by a UV/Vis spectrophotometer at 272 nm. The drug loading content and entrapment efficiency were calculated using the following equations:

$$\text{Loading content (\%)} = \frac{(\text{Weight of IBU in mesoporous material})}{(\text{Weight of mesoporous material loaded with IBU})}$$

$$\text{Entrapment efficiency (\%)} = \frac{(\text{Weight of IBU in mesoporous material})}{(\text{Initial weight of IBU})}$$

#### 2.2.4. Drug release

The release behavior of the IBU loaded SBA-15 and M-SBA-15 was investigated by soaking the tablet of

samples in a solution of simulating body fluid (SBF) at pH 7.4. To avoid limitation of the delivering rate due to external diffusion constraints, continuous stirring was maintained during the assays. 3.0 mL of the suspension was withdrawn at a predetermined time after standing without stirring for 5 min, and the concentration of IBU in the suspension was measured by using a UV/Vis spectrophotometer at 272 nm. After the measurement, the withdrawn suspension was added back to the SBF solution, meanwhile stirring continued. The determination of IBU release in the suspension was repeated for two times and cumulative concentration values of released IBU were obtained.

### 3. RESULTS AND DISCUSSION

The small angle X-ray diffraction patterns of the non-modified SBA-15 and magnetically functionalized sample are shown in Figure 1. The existence of an intense peak at  $2\theta = 0.72^\circ$  and two weak peaks in the  $2\theta$  range of  $1.3^\circ$ - $1.8^\circ$  matches well with the pattern of SBA-15 that reported in the literature [17]. These peaks are attributed to (100), (110) and (200) reflections, respectively that is characteristic of the ordered structure of hexagonal lattice [18]. The intensity of the diffraction peaks decreased after the functionalization due to the existence of magnetic nanoparticles of  $\text{CoFe}_2\text{O}_4$  in the mesochannels.

Figure 2 shows wide-angle X-ray diffraction pattern of M-SBA-15 sample. The observed peaks at 30.51,

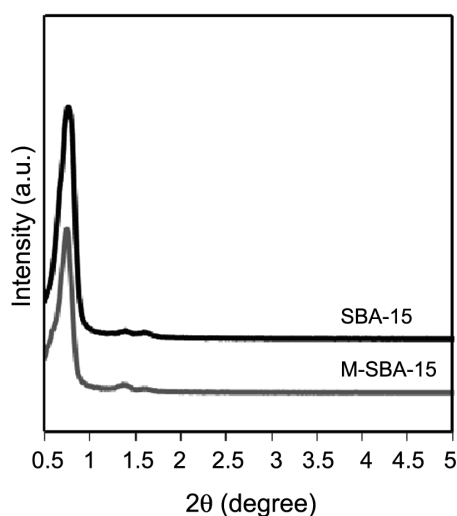


Figure 1: SAXS patterns of SBA-15 and M-SBA-15.

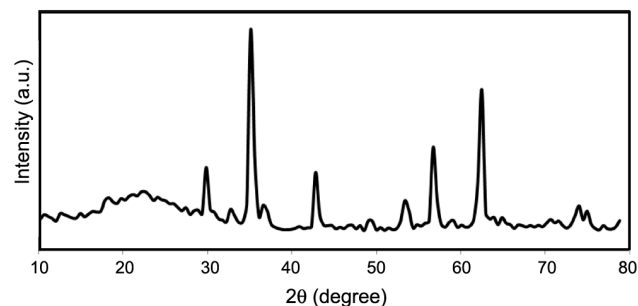


Figure 2: Wide-angle XRD pattern of M-SBA-15 sample.

35.51, 43.21, 57.21, and 62.71 are typically indexed to the crystal phase of  $\text{CoFe}_2\text{O}_4$ .

The morphology of SBA-15 particles before and after modification and drug loading were shown in Figure 3. As it can be observed, the width and length of the twisted particles are about 2 and 30-50  $\mu\text{m}$ , respectively. In addition, the morphology of SBA-15 particles can be maintained unchanged after the magnetization and drug loading.

The  $\text{N}_2$  adsorption/desorption isotherms of two sam-

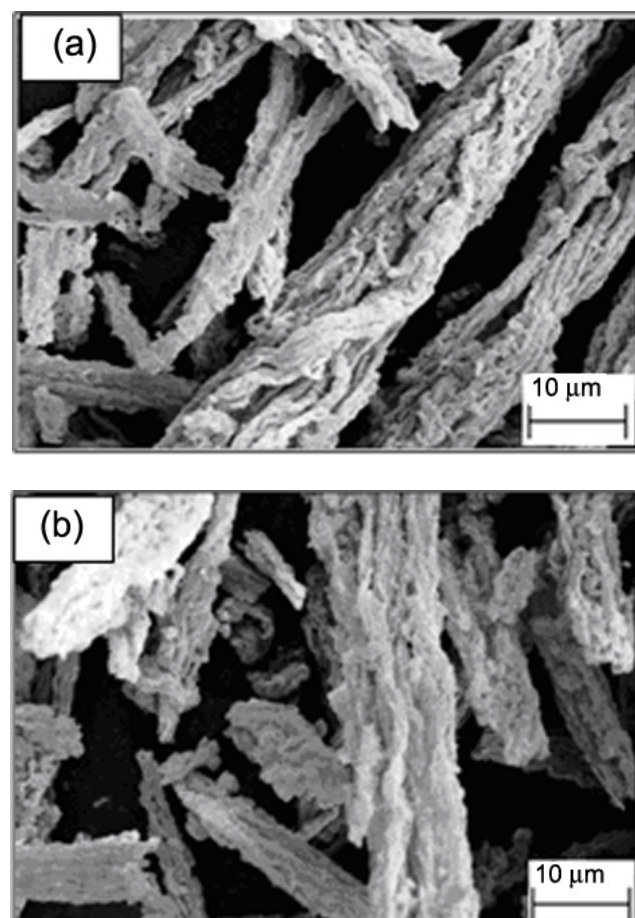
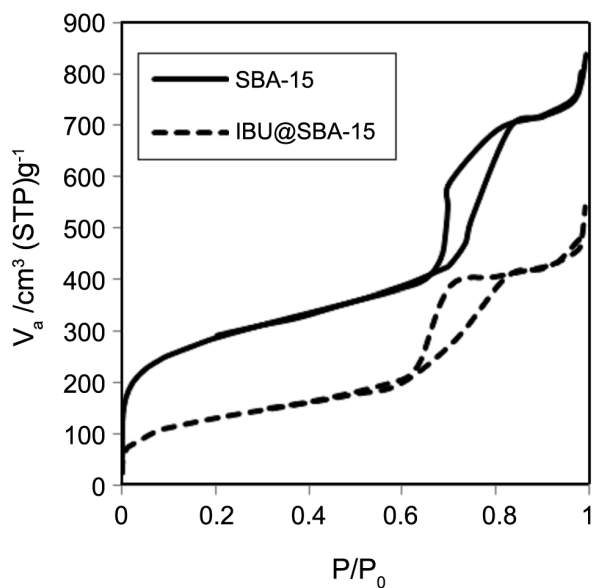
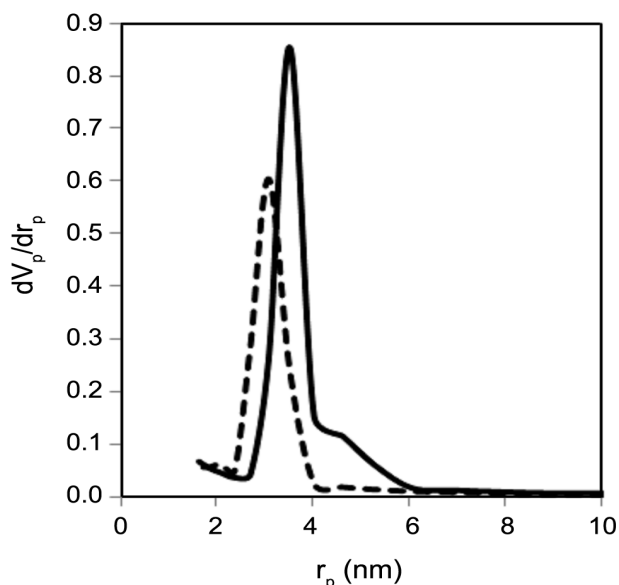


Figure 3: SEM images of (a) non-modified SBA-15 and (b) IBU loaded M-SBA-15.



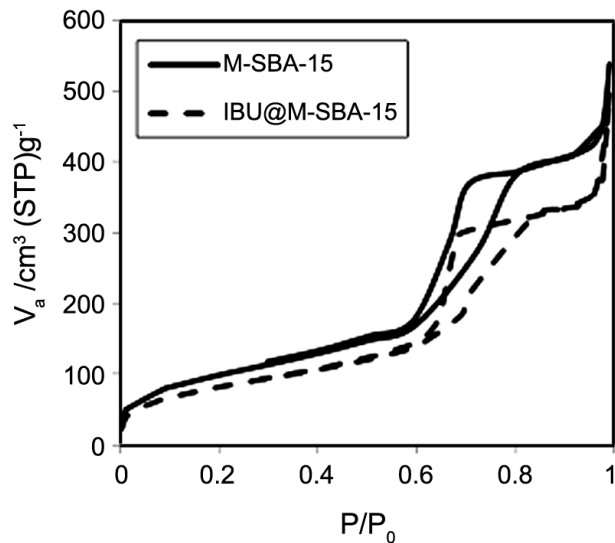
(a)



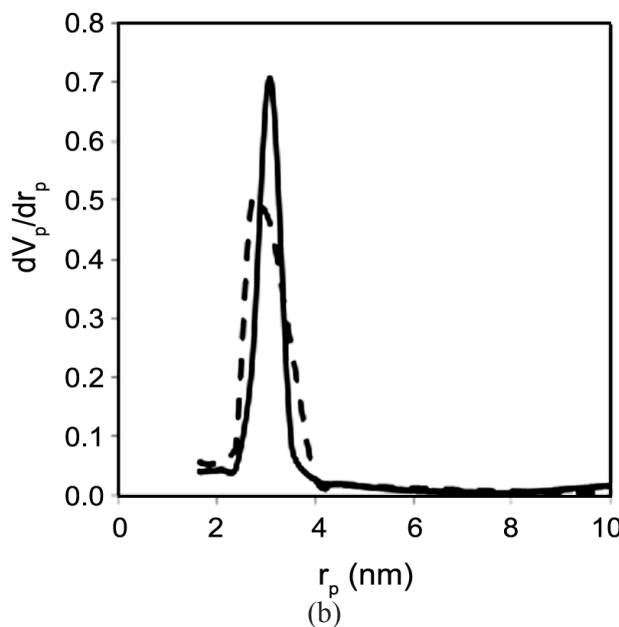
(b)

**Figure 4:** (a)  $N_2$  adsorption/desorption isotherms and (b) pore size distributions of the non-modified SBA-15 before and after IBU loading.

ples before and after IBU loading show a similar trend (Figures 4 and 5). Type IV isotherms with H1 type of hysteresis loops for all samples are observed [19]. The shape and the position of hysteresis loop (at  $p/p_0$  from 0.60 to 0.85) are indicative of narrow mesopore size distribution of the synthesized SBA-15 and its modified samples [20]. The lower amount of adsorbed nitrogen and the shift of hysteresis loop of the functionalized and ibuprofen loaded samples toward lower relative pressures are the indication of the presence of



(a)



(b)

**Figure 5:** (a)  $N_2$  adsorption/desorption isotherms and (b) pore size distributions of the M-SBA-15 before and after IBU loading.

magnetic nanoparticles and drug in the pores. As it is shown in Table 1, the specific surface area ( $S_{BET}$ ), pore volume ( $V_p$ ) and pore diameter ( $D_p$ ) of the modified samples were reduced after the functionalization and loading of ibuprofen.

The pore size distribution was calculated by BJH method base on the desorption branch of  $N_2$  adsorption/desorption isotherms. It is observed that all the samples have narrow pore size distribution with uniform mesochannels.

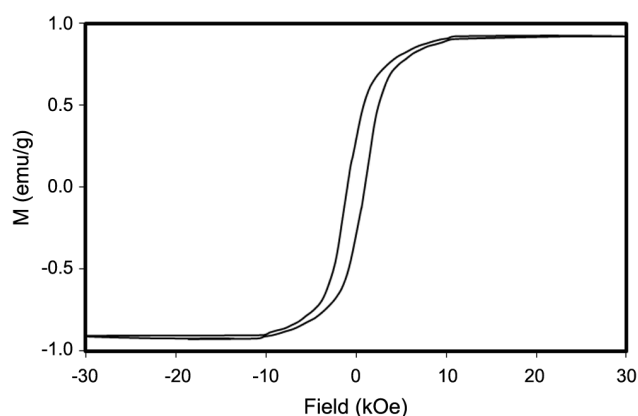
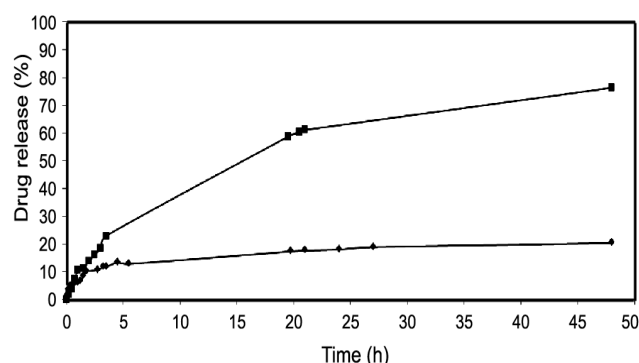
Figure 6 shows the magnetic properties of the

**Table 1:** Textural properties of the non-modified SBA-15, M-SBA-15 and ibuprofen loaded samples.

Sample	$S_{\text{BET}}$ ( $\text{m}^2\text{g}^{-1}$ )	$V_p$ ( $\text{cm}^3\text{g}^{-1}$ )	$D_p$ (nm)
15-SBA	788	1.17	7.1
15-SBA-M	378	0.82	7.0
15-IBU@SBA	311	0.76	6.2
15-SBA-IBU@M	268	0.61	5.4

M-SBA-15 sample. High saturation magnetization (4.3 emu/g) can be observed for this sample.

The magnetic separability of modified SBA-15 was tested by placing a magnet near the glass bottle of sample. The powder of M-SBA-15 is absorbed by the magnet, indicating that M-SBA-15 has a magnetic separability from system. The obtained drug loading capacity and entrapment efficiency of SBA-15 and its magnetically functionalized sample are 30% and 45%, respectively. The drug release behavior of IBU@SBA-15 and IBU@M-SBA-15 was studied in SBF buffer with pH value of 7.4. Figure 7 displays the drug release profile of these samples. In the case of the non-modified SBA-15, 26% of drug was released after 5 h while, in the same period of time, only 12% of IBU was released through M-SBA-15. During next 20 h, in contrast with SBA-15 that the percentage of released drug has shown a flying increase and could reach up to 60%, for M-SBA-15 this percentage is less than 18%. The drug release has stopped through the M-SBA-15 after 48 h but it has continued from the non-modified SBA-15. These results reveal that the rate and amount of released drug decrease after magnetically functionalization. It is may be due to the strong interaction between IBU and magnetic  $\text{CoFe}_2\text{O}_4$  nanoparticles.

**Figure 6:** VSM curve of M-SBA-15.**Figure 7:** Ibuprofen release profile of SBA-15 (◆) and M-SBA-15 (■)

#### 4. CONCLUSIONS

In summary, we have demonstrated the synthesis of a drug delivery system based on SBA-15 with magnetic nanoparticles of  $\text{CoFe}_2\text{O}_4$ . Ibuprofen as a model drug was introduced in the non-modified and functionalized samples. The obtained results of IBU loading and release illustrated the system had a potential use for controlled release. The magnetically functionalized sample due to the stronger interaction with ibuprofen has slower releasing rate. These findings offer promising perspectives for future applications of mesoporous silica materials in controlled drug delivery systems.

#### ACKNOWLEDGEMENTS

The authors thank the financial support from the University of Tehran.

#### REFERENCES

1. Deng Y.H., Wang C.C., Shen X.Z., Yang W.L., Jin

- L., Gao H. and Fu S.K., *Chem. Eur. J.*, **11** (2005), 6006.
2. Nasongkla N., Shuai X.T., Ai H., Weinberg B.D., Pink J., Boothman D.A. and Gao J.M., *Angew. Chem. Int. Ed.*, **43** (2004), 6323.
  3. Bae Y., Fukushima S., Harada A. and Kataoka K., *Angew. Chem. Int. Ed.*, **42** (2003), 4640.
  4. Guo X., Francis C. and Szoka J.R., *Acc. Chem. Res.*, **36** (2003), 335.
  5. Tourne-Peteilh C., Lerner D.A., Charnay C., Nicole L., Begu S. and Devoisselle J.M., *Chem. Phys. Chem.*, **4** (2003), 281.
  6. Barbe C., Bartlett J., Kong L., Finnie K., Lin H.Q., Larkin M., Calleja S., Bush A. and Calleja G., *Adv. Mater.*, **16** (2004), 1949.
  7. Vallet-Regi M., Ruiz-Gonzalez L., Izquierdo-Barba I., Gonzalez-Callbet J.M., *J. Mater. Chem.*, **16** (2006), 26.
  8. Zhu Y.F., Shi J.L., Shen W.H., Dong X.P., Feng J.W., Ruan M.L. and Li Y.S., *Angew. Chem. Int. Ed.*, **44** (2005), 5083.
  9. Ruiz-Hernandez E., Lopez-Noriega A., Arcos D., Izquierdo-Barba I., Terasaki O. and Vallet-Regi M., *Chem. Mater.*, **19** (2007), 3455.
  10. Kim J., Lee J., Lee J., Yu J., Kim B., An K., Hwang Y., Shin C., Park J., Kim J. and Hyeon T., *J. Am. Chem. Soc.*, **128** (2006), 688.
  11. Lin Y., Hung Y., Su J., Lee R., Chang C., Lin M. and Mou C., *J. Phys. Chem. B*, **108** (2004), 15608.
  12. Lin Yu., Wu S., Hung Y., Chou Y., Chang C., Lin M., Tsai C. and Mou C., *Chem. Mater.*, **18** (2006), 5170.
  13. Zhang L., Qiao S.Z., Cheng L., Yan Z. and Lu G.Q., *Nanotechnology*, **19** (2008), 435608.
  14. Kim J., Kim H.S., Lee N., Kim T., Kim H., Yu T., Song I.C., Moon W.K. and Hyeon T., *Angew. Chem. Int. Edit.*, **47** (2008), 8438.
  15. Badiei A., Haririan I., Jahangir A. and Mohammadi Ziarani G., *Dyn. Biochem. Process Biotech. Mol. Biol.*, (2009), 48.
  16. Du Y., Liu S., Ji Y., Zhang Y., Xiao N. and Xiao F.S., *J. Magn. Magn. Mater.*, **320** (2008), 1932.
  17. Bahrami Z., Badiei A., Atyabi F., *Chem. Eng. Res. Des.*, **92** (2014), 1296.
  18. Yadavi M., Badiei A. and Mohammadi Ziarani G., *Appl. Surf. Sci.*, **279** (2013), 121.
  19. Khaniani Y., Badiei A. and Mohammadi Ziarani G., *J. Mater. Res.*, **27** (6) (2012), 932.
  20. Badiei A., Goldooz H. and Mohammadi Ziarani G., *Appl. Surf. Sci.*, **257** (2011), 4912.